Journal of Organometallic Chemistry 693 (2008) 2597–2602

Contents lists available at ScienceDirect

Journal of Organometallic Chemistry

journal homepage: www.elsevier.com/locate/jorganchem

Syntheses and molecular structures of 18/16-electron half-sandwich iridium(III) complexes with chelating anilido-imine ligands

Xia Meng, Yue-Jian Lin, Guo-Xin Jin *

Shanghai Key Laboratory of Molecular Catalysis and Innovative Materials, Department of Chemistry, Fudan University, Shanghai 200 433, China

ARTICLE INFO

Article history:
Received 18 January 2008
Received in revised form 29 April 2008
Accepted 6 May 2008
Available online 10 May 2008

Dedicated to Herr Professor Dr. Wolfgang A. Herrmann on the occasion of his 60th birthday.

Keywords:
Iridium
Half-sandwich complexes
Anilido-imine ligands
Coordinative unsaturated
Molecular structures

ABSTRACT

A 18-electron complex $Cp^*IrCl[o\text{-}C_6H_4N(C_6H_3\text{-}Me\text{-}p)(CH{=}NC_6H_3\text{-}Me\text{-}p)]$ (Cp^* = η^5-pentamethylcyclopentadienyl) (**1a**) was obtained by the reaction of the lithium salt of $o\text{-}C_6H_4N(C_6H_3\text{-}Me\text{-}p)(CH{=}NHC_6H_3\text{-}Me\text{-}p)$ ($\mathbf{L}_1$) with $[Cp^*IrCl(\mu\text{-}Cl)]_2$ in toluene. However, when bulkier ligands ($\mathbf{L}_2$ = $o\text{-}C_6H_4N(C_6H_3\text{-}Me\text{-}p)(CH{=}NHC_6H_3\text{-}i\text{-}Me_2\text{-}2,6)$, $\mathbf{L}_3$ = $o\text{-}C_6H_4N(C_6H_3\text{-}Me\text{-}p)(CH{=}NHC_6H_3\text{-}i\text{-}Pr_2\text{-}2,6)$) were employed in the same reaction, two 16-electron complexes $\{Cp^*Ir[o\text{-}C_6H_4N(C_6H_3\text{-}Me\text{-}p)(CH{=}NC_6H_3\text{-}i\text{-}Me_2\text{-}2,6)]\}^+Cl^-$ (**2b**) and $\{Cp^*Ir[o\text{-}C_6H_4N(C_6H_3\text{-}Me\text{-}p)(CH{=}NC_6H_3\text{-}i\text{-}Pr_2\text{-}2,6)]\}^+Cl^-$ (**3b**) were formed. A 16-electron complex $\{Cp^*Ir\ [o\text{-}C_6H_4N(C_6H_3\text{-}Me\text{-}p)(CH{=}NC_6H_3\text{-}Me\text{-}p)]\}^+SO_3CF_3^-$ (**1b**) bearing $\mathbf{L}_1$ could be achieved by the reaction of **1a** with $AgSO_3CF_3$ in CH_3CN solution. The molecular structures of **1a** and **2b** were determined by X-ray crystallography. Theoretical calculations of all the 18/16-electron species were performed to study their bonding characters and electronic properties. Electron donating effect of Cp^* and steric effect of anilido-imine ligand were considered as major factors in the formation of coordinative unsaturated complexes **1b**, **2b**, **3b**.

1. Introduction

Coordinative unsaturated complexes have attracted much attention for the amazing chemistry they demonstrate [1,2]. In the past decade, bulky aryl-substituted β-diketimine has been dramatically developed because of its strong electron donation and steric constraints that can stabilize low-coordinate main group and late transition metal complexes such as three coordinated Zn, Cu, Ni, Ga complexes [3]. Chelating anilido-imine (AnIm) ligand has similar steric and electronic features with β-diketimine, and a rigid framework could protect the ligand backbone from α-carbon attack which brings complexity to the products [4]. Since 2003, complexes containing AnIm ligand was synthesized, some of them shown excellent properties of fluorescence emission, such as Y, Al, B complexes, *etc.* [4a,4e,4f,4i], others were used as ancillary ligands for the mechanism and dynamic studies to stabilize reaction intermediates [4c,4h]. At the same time, iridium complexes have long been considered as a promising catalyst for many organic reactions [5], for example for ketone and aldehyde hydrogenation, alcohol dehydrogenation and C–H bond activation to synthesize organic compounds. Thus, the building of half-sandwich iridium complex with a proper ancillary ligand is an interesting and important subject. In this report, half-sandwich iridium complexes with AnIm ligand were synthesized (Scheme 1) and coordinative unsaturated complexes were obtained when bulky substitute AnIm were involved. Some detailed studies on these 18/16-electron complexes were performed to explore their electronic and steric features.

2. Results and discussion

2.1. Syntheses of complexes

Anilido-imine ligands *ortho*-C_6H_4 ($NHAr_1$)($CH{=}NAr_2$) $\mathbf{L}_1$–$\mathbf{L}_5$ were prepared in good yields by the reaction of *ortho*-$C_6H_4F(CH{=}NAr_2)$ with corresponding $LiN(H)Ar_1$ (Scheme 2) according to the literature [6]. These ligands were characterized by ^1H NMR and IR spectroscopy. The NH resonances characteristically appear at low field. The IR absorption bands of the imine C=N stretch occur in the region 1620–1623 cm^{-1} [5,6]. After the AnIm ligands $\mathbf{L}_1$–$\mathbf{L}_3$ were treated with *n*-BuLi to give corresponding lithium salts in toluene solution, 1/2 equiv. of $[Cp^*IrCl(\mu\text{-}Cl)]_2$ was added to give a dark red solution, and iridium complexes **1a**, **2b** and **3b** were obtained in relatively high yields. (1) All the complexes were air stable in solid state and well soluble in hexane. X-ray crystallographic analysis confirms that **1a** is an 18-electron half-sandwich complex, while **2b** which contains a bulkier ligand is an unexpected 16-electron complex. However, when ligands $\mathbf{L}_4$ and $\mathbf{L}_5$ were treated with the same procedure, only starting materials were separated after reaction. This sug-

* Corresponding author. Tel.: + 86 21 65643776; fax: +86 21 65641740.
E-mail address: gxjin@fudan.edu.cn (G.-X. Jin).

0022-328X/$ - see front matter © 2008 Elsevier B.V. All rights reserved.
doi:10.1016/j.jorganchem.2008.05.002

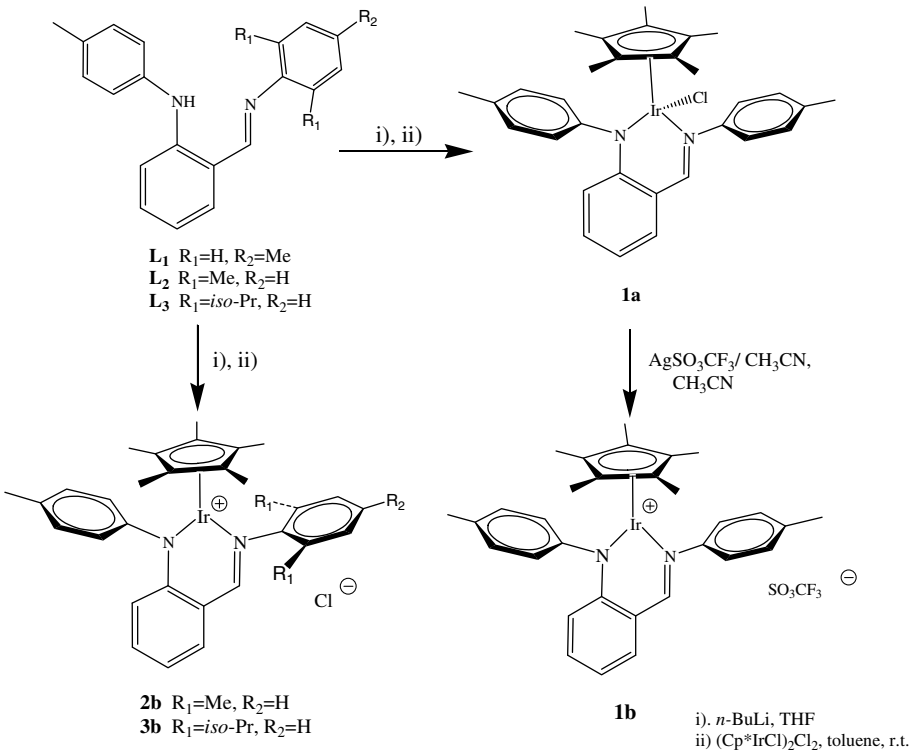

L1 R1=H, R2=Me
L2 R1=Me, R2=H
L3 R1=iso-Pr, R2=H

Scheme 1. Synthesis of complexes **1a**, **1b**, **2b** and **3b**.

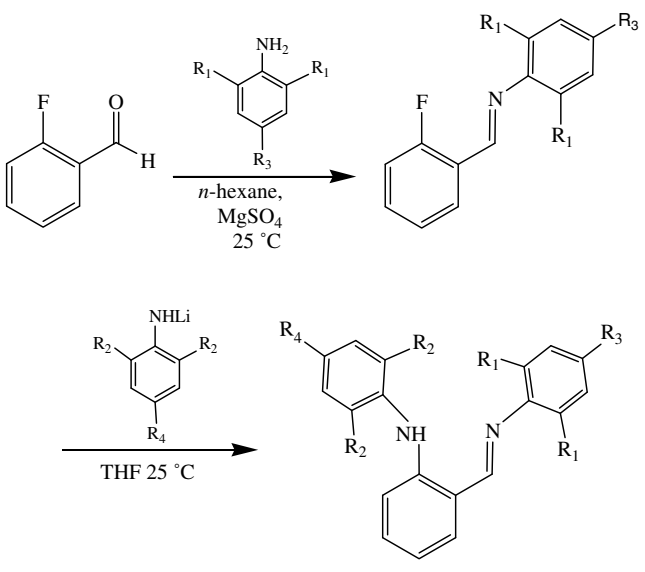

L1, R1=R2=H, R3=R4=Me
L3, R1=*i*-Pr, R2=R3=H, R4=Me
L5, R1=R2=*i*-Pr, R3=R4=H
L2,R1=Me,R2= R3=H, R4=Me
L4, R1=R2=Me, R3=R4=H

Scheme 2. Synthesis of ligands L_1–L_5.

gests that bulky groups at phenyls which connect to the amido and imino nitrogen atoms in the AnIm ligands greatly affect the formation and stability of the expected products. A 16-electron complex with L_1 could be achieved by changing Cl^- into a larger anion. When $AgSO_3CF_3$ solution in CH_3CN was added into a solution of **1a** in toluene, bright red complex **1b** was obtained and characterized by ^1H NMR and elemental analysis.

The ^1H NMR of **1a**, **2b** and **3b** show C*H*=N resonances at *ca.* 8.82–8.84 ppm. The hydrogen at Cp^* of **1a** and **2b** is at a high field of 1.16–1.18 ppm as a single signal, but the hydrogen of Cp^* from **3b** shift to a lower field at 1.52 ppm, indicating a remarkable repulsion between Cp^* and AnIm ligand which reduces the overlap between Cp^* and the metal center. The H atoms on methyl and isopropyl which connect to the phenyl at imine nitrogen split into two and four sets respectively, indicating that there is no mirror plane in the molecules. Compared with the 18-electron complex **1a**, almost all the hydrogen in 16-electron complex **1b** slightly shift into lower field, due to the positive charge it takes. The IR absorption bands of the imine C=N stretch blue shift to the region 1610–1600 cm^{-1} in comparison with the free ligands at about 1620 cm^{-1} [6].

2.2. Crystal Structures

Single crystals of complexes **1a** and **2b** suitable for X-ray crystallographic analysis were obtained by recrystallization of solvent from *n*-hexane and toluene solution at low temperature, respectively. The ORTEP diagrams of the molecular structures of these complexes are shown in Figs. 1 and 2. Crystallographic data for **1a** and **2b** are summarized in Table 1. **1a** and **2b** were crystallized in the monoclinic space group $P2_1/n$. Molecular structure analysis reveals that **1a** is neutral 18-electron species containing a chelating anilido-imine ligand, a η^5-Pentamethylcyclopentadiene (Cp^*) group and a chloride, while **2b** is a 16-electron cation with a chloride as equilibrium ion. The metal center of complex **1a** adopts distorted three-leg piano stool geometry [8,9], which is different from the two-legged geometry of **2b**. The dihedral angle between the Ir1–N1–C1–C2–C3–N2 plane and Cp^* is 63.2° for **1a**. But for **2b**, these two planes are almost perpendicular (88.9°). In complex **1a** and **2b**, the six-membered chelating rings are almost in the same plane [5,6]. The aromatic groups connect to the amido and imino nitrogen lie approximately parallel with the Cp^*. The imino C=N

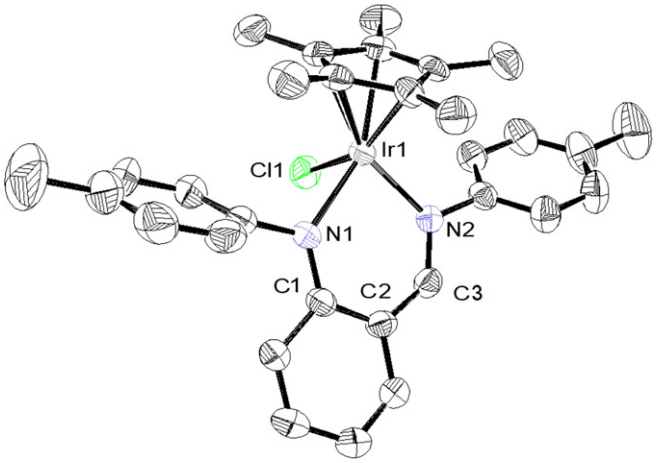

Fig. 1. Thermal ellipsoid plot of **1a** (50% probability thermal ellipsoids). Selected bond lengths (Å) and angles (°): Ir1–N2 2.085(4), Ir1–N1 2.106(4), Ir1–Cl1 2.489-0(13), N1–C1 1.356(6), N2–C3 1.299(6), N2–Ir1–N1 87.96(15), N2–Ir1–Cl1 84.54 (11), N1–Ir1–Cl1 85.56(12).

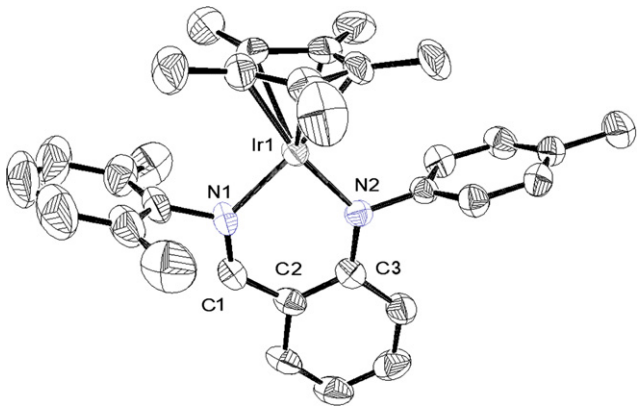

Fig. 2. Thermal ellipsoid plot of **2b** (50% probability thermal ellipsoids). Chloride anion was deleted for clarity. Selected bond lengths (Å) and angles (°): Ir1–N2 1.976(4), Ir1–N1 2.007(4), N1–C1 1.294(7), N2–C7 1.370(6), Ir1–C23 2.164(5), Ir1–C25 2.175(6), Ir1–C26 2.199(6), Ir1–C27 2.217(6), Ir1–C24 2.221(5), N2–Ir1–N1 88.34(17).

bonds retain their double bond character which have already been reported in the complexes containing AnIm ligand according to the literatures [5,6]. The two Ir–N bonds in **1a** (Ir(1)–N(2), 2.085(4) Å; Ir(1)–N(1), 2.106(4) Å) are distinctly shorter than those bonds in **2b** (Ir(1)–N(2), 1.976(4) Å; Ir(1)–N(1), 2.007(4) Å), due to the stronger electron affinity of the metal center which takes more positive charge in complex **2b**. The Ir–Cl bond in complex **1a** is 2.489 Å aligned with literatures [7,8].

2.3. Absorption spectroscopy and electrochemical properties of *1a*, *1b*, *2b*, and *3b*

The electronic spectrums of **1a**, **1b**, **2b**, and **3b** show three transitions at 270–290 nm, 325–345 nm and 420 nm in CH_2Cl_2. Compared with free ligands, the absorption bands around 280 nm, which could be assigned to the $\pi \rightarrow \pi^*$ transitions, are similar with the bands in free ligands. The absorptions bond at 325–345 nm, which are not observed in free ligands, must be assigned to the $\pi \rightarrow \pi^*$ transition of Cp^* and the broad moderate intense absorptions at 400–500 nm may receive contribution mainly from $\pi \rightarrow \pi^*$ transition of chelating ligands [4e,4i], LMCT and d → d transition of the metal center. Besides, the similarity of absorption bands of 18 and 16 electron complexes suggests that the electronic features of these complexes are similar (see Fig. 3).

Table 1
Crystallographic data for **1a** and **2b**

Formula	$C_{31}H_{34}ClIrN_2$ (**1a**)	$C_{32}H_{36}ClIrN_2$ (**2b**)
Unit cell	Monoclinic	Monoclinic
Formula weight	662.25	676.28
Space group	*P*2(1)/*c*	*P*2(1)/*c*
a (Å)	11.482(3)	21.019(7)
b (Å)	27.835(7)	8.143(3)
c (Å)	8.634(2)	20.698(7)
Volume (Å^3)	2734.9(1)	3161.3(2)
α (°)	90	90
β (°)	97.647(4)	116.826(4)
γ (°)	90	90
Z	4	4
Temperature (K)	293(2)	293(2)
μ (Mo Kα) (A)	0.71073	0.71073
Density (mg/m^3)	1.608	1.421
R_1[a] [$I > 2\sigma(I)$]	0.0301	0.0400
wR_2[b]	0.0628	0.0899
Goodness-of-fit on F^2	1.062	0.939

[a] $R_1 = \sum(||F_o| - |F_c||)/\sum|F_o|$.
[b] $wR_2 = [\sum(|F_o|^2 - |F_c|^2)^2/\sum(F_o^2)]^{1/2}$.

The cyclic voltammetery studies of complex **1a** shows a quasi-reversible reduction wave at −1.09 V which can be assigned to the reduction process of **1a** → **1a**$^-$ [10]. However, complexes **1b**, **2b** and **3b** present irreversible reductive waves at −1.00 V, −1.06 V and −1.10 V. The wave declined quickly after several laps, indicating **1b**$^-$, **2b**$^-$ and **3b**$^-$ are unstable species. The different electrochemical behaviors can be explained by different HOMO and LUMO characters in 16 and 18 electron complexes. All the compounds $\mathbf{L}_1$, $\mathbf{L}_2$, and $\mathbf{L}_3$ do not show any distinct reductive waves in the experiment.

2.4. Theoretical calculations

DFT calculation was performed [11,12] in order to study the electronic properties of complexes **1a**, **1b**, **2b** and **3b**, and find out why coordinative unsaturated complexes could be stabilized by AnIm ligands. Geometry optimization of the singlet state of the complexes **1a** and **2b** led to similar structures which were in good agreement with experimental data. Structures of **1b** and **3b** were built on the basis of **2b** and optimized for comparison. 18-electron structure of **3b** build on the basis of **1a** was proved to be an unstable conformation during the geometry optimization. **1b**, **2b** and **3b** have similar configuration and HOMO/LUMO distribution. The orbital energy diagram for the frontier orbits of complex **1a**, **1b** and **2b** is shown in Fig. 4. The three complexes have similar energy gap between HOMO and LUMO. But the HOMO and LUMO of **1a** are about 4.7 eV higher than those of **1b** and **2b**. In complex **1b** and **2b**, the frontier orbits are mainly comprised of contributions from the d_{xz}, d_{yz} orbits of Ir, p_z orbits of N1, N2, and p_z orbits associated with other atoms of the chelating ligand.

From the orbital diagram, we can infer that, in the 16-electron complex **2b**, HOMO is a bonding combination originating mainly from AnIm ligands with a small metal contribution. And LUMO mainly locates on the iridium atom and Cp^* group with strong bonding character, but shows anti-bonding character between Ir and AnIm ligand. However, in the 18-electron complex **1a**, HOMO has a anti-bonding character and LUMO has a weak bonding character between the Ir and N. The different feature of frontier orbits between **1a** and **2b** gives us an explanation of the different cyclic voltammetery behavior which has been mentioned previously. Adding an electron to the LUMO of **1a** will slightly intensify the bond between Ir

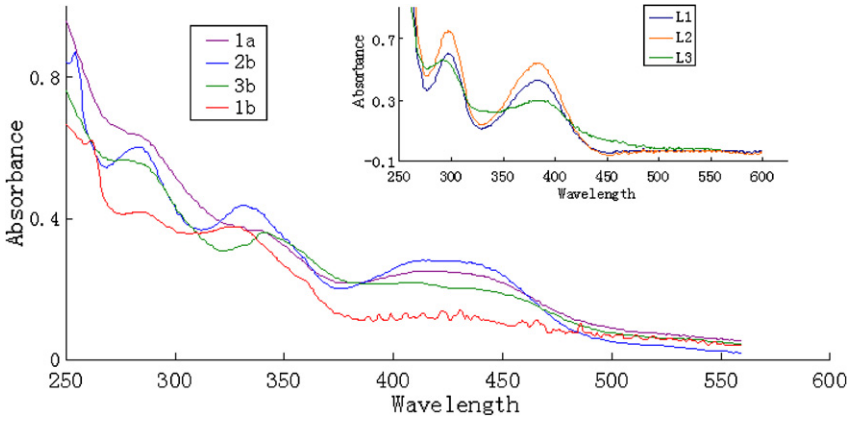

Fig. 3. UV–Vis spectra of **1a**, **1b**, **2b**, **3b**, L_1, L_2, and L_3 in CH_2Cl_2.

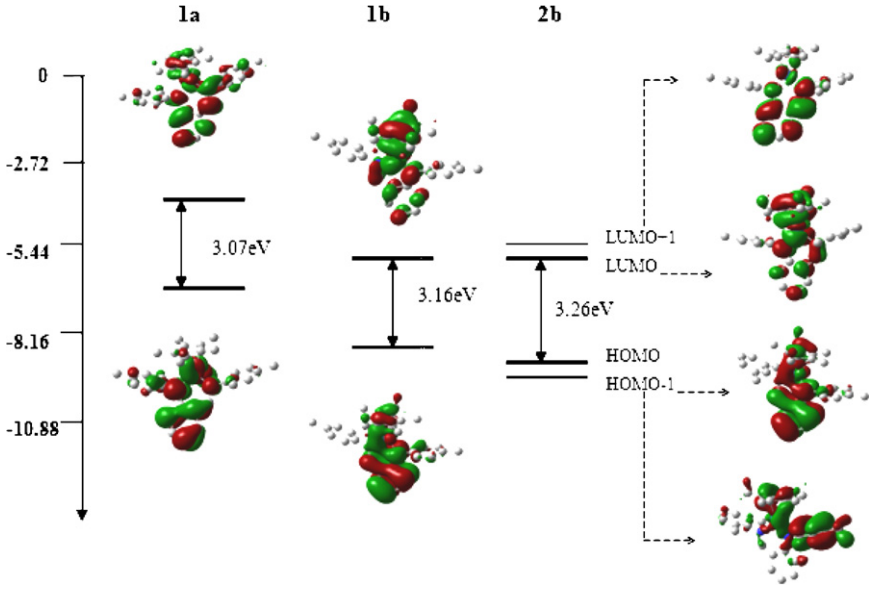

Fig. 4. Orbital energy diagram for the frontier orbitals of **1a**, **1b** and **2b**.

Table 2
Calculated atomic charge distribution of the studied complexes

	Ir	Cp^*	Anilido-imine
1a	0.24	0.37	−0.28
1b	0.46	0.59	−0.05
2b	0.43	0.60	−0.03
3b	0.36	0.61	0.03

and AnIm ligand, making the Ir (II) species stable. But adding an electron to the anti-bonding LUMO of **2b** will strongly weaken the Ir–AnIm bond, leading to ligand decomposition.

Mulliken atomic charge distributions on Ir, Cp^* and anilido-imine ligand of complexes **1a**, **1b**, **2b** and **3b** are listed in Table 2. Cp^* shares more than half of the positive charge in all complexes. This can be explained as efficient d–π overlap between Ir and Cp^* and π-back donation from Cp^* to Ir. In contrast, due to the poor bonding orbit between Ir and AnIm, the positive charge on iridium does not efficiently shared by AnIm. Thus, we can infer that, in the formation of 16-electron species, Cp^* contributes as an electron donating group to share positive charge of the complex, and the AnIm behaves as a bulky ancillary ligand to protect the metal center from outside attack.

3. Conclusion

In this work, we have reported novel 18/16-electron iridium complexes **1a**, **1b**, **2b** and **3b** containing anilido-imine and Cp^* ligand. Crystal structures of **1a** and **2b** have been determined. All of these complexes were studied by IR, ^1H NMR, UV–Vis spectra, elemental analyses, and cyclic voltammetery. DFT calculation helps us to understand the electronic feature of these coordinate unsaturated complexes. Different frontier orbit distribution of the 18 and 16 electron complexes affect their electrochemical properties. It is believed that the combination of electron donation from Cp^* and bulky substitution of AnIm ligand contribute to the stabilization of 16-electron complex. A deep understanding on this subject may help us to design and develop new complexes with controllable electronic and steric factors.

4. Experimental

4.1. General procedures

All manipulations of air- and/or water-sensitive compounds were carried out under nitrogen using standard Schlenk techniques. Solvents were dried by refluxing with appropriate drying agents and distilled under nitrogen prior to use. All chemicals which were commercially available were used without further purification. The starting material $[Cp^*IrCl(\mu\text{-}Cl)]_2$ was prepared according to literature methods [6]. ^1H NMR spectra were recorded with a Varian Unity-400 spectrometer. Elemental analyses were performed on an Elementarvario EL III Analyzer. Cyclic voltammetry (CV) was carried out on CH Instruments electrochemical workstation (model 600A) at a scanning rate of 50 mV/s. Complex **1a** was dissolved in CH_2Cl_2 using 0.1 M $N(nBu)_4PF_6$ as the supporting electrolyte [10]. UV spectra were recorded at room temperature with an Agilgent instrument 8543.

4.2. Synthesis of o-C_6H_4NH (C_6H_3-Me-p)(CH=NC_6H_3-Me-p) (**L_1**)

Ligands $\mathbf{L_1}$–$\mathbf{L_5}$ were prepared in good yields according to the literature without major modification, (2). Herein the synthesis of $\mathbf{L_1}$ will be taken as an example. A mixture of *ortho*-fluorobenzaldehyde (5.0 mL, 47.1 mmol), *p*-toluidine (5.0 g, 47.1 mmol), and $MgSO_4$ (1.0 g) in *n*-hexane (30 mL) was stirred for 2 h. The mixture was filtered, and the yellow solid *ortho*-$C_6H_4F(CHNC_6H_4Me\text{-}p)$ was obtained after the solvent was removed, Pure product was obtained by recrystallization from hexane. A solution of *n*-BuLi (19.0 mL, 30.4 mmol) in hexanes was added to a solution of 2,6-dimethylaniline (5.0 mL, 30 mmol) in THF (20 mL) at −78 °C. The reaction mixture was warmed to room temperature and stirred overnight. The resulting solution of LiNHAr was transferred into a solution of *ortho*-$C_6H_4F(CHNC_6H_4Me\text{-}p)$ (6.39 g, 30 mmol) in THF (20 mL) at 25 °C. After stirring for 1 h, the reaction was quenched with 10 mL H_2O, the mixture was extracted with *n*-hexane, and the organic phase was evaporated to vacuo to give a yellow solid crude product. Pure product was obtained as yellow crystals by recrystallization from methanol. (5.4 g, 56%). Anal. Calc. for $C_{21}H_{20}N_2$ (300.4): C, 83.96; H, 6.71; N, 9.33. Found: C, 83.76; H, 6.91; N, 9.27%. ^1H NMR ($CDCl_3$): δ 11.15 (s, 1H, NH), 8.59 (s, 1H, CH=NAr), 7.40 (d, 1H, Ph–H), 7.28–7.12 (m, 10H, Ph–H), 6.77 (t, 1H, Ph–H), 2.37 (s, 3H, CH_3), 2.35 (s, 3H, CH_3). IR (KBr): 3200(w), 3072(w), 3011(w), 2914(s), 2878(s), 1617(s), 1594(s), 1566(s), 1518(s), 1452(s), 1325(m), 1181(m), 1155(m), 827(m), 750(m), 517(m) cm^{-1}.

The ligands $\mathbf{L_2}$–$\mathbf{L_5}$ were synthesized by the similar procedure with $\mathbf{L_1}$, and all the ^1H NMR resonances of these ligands were in good accordance with the literatures.

o-C_6H_4NH (C_6H_3-Me-p)(CH=NC_6H_3-Me_2-2,6) (**L_2**): Anal. Calc. for $C_{22}H_{22}N_2$ (314.4): C, 84.04; H, 7.05; N, 8.91. Found: C, 83.95; H, 6.95; N, 8.90%. ^1H NMR ($CDCl_3$): δ 11.07 (s, 1H, NH), 8.32 (s, 1H, CH=NAr), 7.32–7.08 (m, 9H, Ph–H), 6.95 (m, 1H, Ph–H), 6.79 (m, 1H, Ph–H), 2.34 (s, 3H, $PhCH_3$), 2.19 (m, 6H, Ph–CH_3). IR (KBr): 3208(w), 3067(w), 3020(w), 2946(m), 2915(m), 2859(s), 2859(w), 1620(s), 1584(s), 1572(s), 1518(s), 1456(s), 1374(m), 1328(s), 1216(w), 1175(m), 1159(m), 1117(w), 1089(m), 1042(w), 910(m), 859(w), 831(m), 801(w), 770(m), 754(m), 616(m) cm^{-1}.

o-C_6H_4NH (C_6H_3-Me-p)(CH=NC_6H_3-*i*-Pr_2-2,6) (**L_3**): Anal. Calc. for $C_{26}H_{30}N_2$ (370.5): C, 84.28; H, 8.16; N, 7.56. Found: C, 84.20; H, 8.31; N, 7.35%. ^1H NMR ($CDCl_3$): δ 11.05 (s, 1H, NH), 8.30 (s, 1H, CH=NAr), 7.33 (t, 2H, Ph–H), 7.27 (m, 1H, Ph–H), 7.19–7.13 (m, 7H, Ph–H), 6.80 (t, 1H, Ph–H), 3.05(m, 2H, $CH(CH_3)_2$), 2.34(s, 3H, $PhCH_3$), 1.19–1.17 (m, 12H, $CH(CH_3)$). IR (KBr): 3200(w), 3060(w), 2919(m), 2867(s), 1619(s), 1596(s), 1571(s), 1527(s), 1461(s), 1377(w), 1329(s), 1253(w), 1209(w), 1171(m), 1116(w), 1034(m), 914(m), 860(w), 817(w), 799(m), 742(m), 645(w) cm^{-1}.

4.3. Synthesis of Cp^*IrCl[o-C_6H_4N(C_6H_3-Me-p)(CH=NC_6H_3-Me-p)] (**1a**)

A solution of *n*-BuLi (1.6 M, 0.28 mL, 0.45 mmol) in hexane was added dropwise to a stirred solution of ligand $\mathbf{L_1}$ (0.123 g, 0.41 mmol) in THF (10 mL) at −78 °C. The mixture was slowly warmed to room temperature and stirred for 3 h. The solvent was removed under vacuum, and toluene (10 mL) was added to the solid residue. The resultant mixture containing the lithium salt of $\mathbf{L_1}$ was slowly channeled to a suspension of $(Cp^*IrCl_2)_2$ (0.16 g, 0.2 mmol) in toluene (10 mL) and continuously stirred overnight at room temperature. A dark red suspension was allowed to stand for 1 day, and LiCl was removed by filtration. The solution was concentrated to about 3 mL, and cooled to −30 °C to obtain dark red solid. Small red crystals were obtained through recrystallization from hexane (0.19 g, 70%). Anal. Calc. for $C_{31}H_{34}ClIrN_2$ (662.25): C, 56.22; H, 5.17; N, 4.23. Found: C, 56.65; H, 4.91; N, 3.87%. ^1H NMR (400 MHz, $CDCl_3$, 293 K): δ 8.84 (s, 1 H, CH=NAr), 7.55 (d, H, Ph–H), 7.42–7.39 (m, 8H, Ph–H), 7.15 (t, 1H, Ph–H), 7.08 (d, 1H, Ph–H), 6.60 (d, 1H, Ph–H), 2.52 (d, 6H, Ph–CH_3), 1.18 (s, 15H, Cp-5CH_3) ppm. IR (KBr): 3052(w), 3011(w), 2914(s), 2860(s), 1612(s), 1591(s), 1503(s), 1496(m), 1436(m), 1372(w), 1338(m), 1165(m), 1104(m), 1026(m), 803(m), 742(m), 496(w) cm^{-1}.

4.4. Synthesis of Cp^*Ir[o-C_6H_4N(C_6H_3-Me-p)(CH=NC_6H_3-Me-p)] SO_3CF_3 (**1b**)

A solution of $AgSO_3CF_3$ (0.12 M, 1.6 mL, 0.2 mmol) in CH_3CN was added dropwise to a stirred solution of **1a** (0.133 g, 0.2 mmol) in toluene (10 mL) at room temperature. The mixture was stirred for another 2 h, when the color gradually turned from dark red to red. The solution was filtered to remove AgCl, and the solvent was evaporated under vacuum to yield **2a** (85%). Anal. Calc. for $C_{32}H_{34}F_3IrN_2O_3S$ (775.9): C, 49.53; H, 4.42; N, 3.61; S, 4.13. Found: C, 50.01; H, 4.04; N, 3.84; S, 3.87%. ^1H NMR (400 MHz, $CDCl_3$, 293 K): δ 9.00 (s, 1H, CH=NAr), 7.67 (d, 1H, Ph–H), 7.47–7.16 (m, 9H, Ph–H), 7.00 (d, 1H, Ph–H), 6.71 (d, 1H, Ph–H), 2.58 (d, 3H, Ph–CH_3), 2.52 (d, 3H, Ph–CH_3), 1.18 (s, 15H, Cp-5CH_3) ppm. IR (KBr): 3026(w), 2918(s), 1610(s), 1575(s), 1536(s), 1504(m), 1454(m), 1270(s), 1222(m), 1148(s), 1030(s), 869(m), 762(m) cm^{-1}.

4.5. Synthesis of Cp^*Ir[o-C_6H_4N(C_6H_3-Me-p)(CH=NC_6H_3-*i*-Me_2-2, 6)]Cl (**2b**)

Complex **2b** was obtained in a similar strategy to that used in the isolation of **1a** (0.10 g, 75%). Anal. Calc. for $C_{32}H_{36}ClIrN_2$ (676.28): C, 56.83; H, 5.37; N, 4.14. Found: C, 56.65; H, 4.99; N, 3.81%. ^1H NMR (400 MHz, $CDCl_3$, 293 K): δ 8.82 (s, 1H, CH=NAr), 7.69 (d, H, Ph–H), 7.55 (d, 1H, Ph–H), 7.47–6.70 (m, 9H, Ph–H), 2.59 (d, 3H, Ph–CH_3), 2.20 (d, 6H, Ph-2CH_3), 1.16 (s, 15H, Cp-5CH_3) ppm. IR (KBr): 3388(m), 3072(s), 3061(s), 2960(m), 2865(w), 1600(s) 1505(s), 1499(s), 1447(m), 1404(m), 1326(s), 1179(m), 906(m), 768(m) cm^{-1}.

4.6. Synthesis of Cp^*Ir[o-C_6H_4N(C_6H_3-Me-p)(CH=NC_6H_3-*i*-Pr_2-2,6)]Cl (**3b**)

Complex **3b** was obtained in a similar strategy to that used in the isolation of **1a** (0.10 g, 75%). Anal. Calc. for $C_{35}H_{42}ClIrN_2$ (732.28): C, 59.04; H, 6.06; N, 3.82. Found: C, 58.64; H, 6.44; N, 3.62%. ^1H NMR (400 MHz, $CDCl_3$, 293 K) δ8.82 (s, 1H, CH=NAr), 7.82 (d, H, Ph–H), 7.42–7.10 (m, 9H, Ph–H), 6.62 (d, 1H, Ph–H),

6.51 (d, 1H, Ph–H) 6.04 (d, 1H, Ph–H), 5.66 (t, 1H, Ph–H), 5.29 (s, 1H, Ph–H), 3.67 (p, 1H, C*H*(CH_3)$_2$), 3.56 (p, 1H, C*H*(CH_3)$_2$), 2.33 (s, 3H, Ph–CH_3), 1.52 (s, 15H, Cp-5CH_3), 1.32 (d, 1H, CH(C*H*$_3$)$_2$), 1.26 (d, 1H, CH(C*H*$_3$)$_2$), 1.14 (d, 1H, CH(C*H*$_3$)$_2$), 0.88 (d, 1H, CH(C*H*$_3$)$_2$) ppm. IR (KBr): 3388(m), 3073(s), 2961(m), 2918(w), 2867(s), 1599(s) 1505(s), 1447(m), 1402(s), 1311(s), 1218(m), 1149(m), 1089(m), 1029(m), 938 m), 881(m) cm^{-1}.

4.7. X-ray structure determinations of **1a** and **2b**

Single crystals of **1a** and **2b** suitable for X-ray structural analysis were obtained from *n*-hexane and toluene. The intensity data of the single crystal were collected on the CCD-Bruker Smart APEX system [12]. All determinations of the unit cell and intensity data were performed with graphite-monochromated Mo Kα radiation (λ = 0.71073 Å) at room temperature. These structures were solved by direct methods, using Fourier techniques, and refined on F^2 by full matrix least-squares method. All the non-hydrogen atoms were refined anisotropically, and all the hydrogen atoms were included but not refined. Details of the data collection and refinement are summarized in Table 1.

4.8. Density functional theory (DFT) calculations

The structure of **1a** and **2b** was optimized for the singlet state using the DFT method with B3LYP functional in the gas phase in the GAUSSIAN 03 packages. LANL2DZ basis set was used for Ir, and 6-31G basis set was used for C, N, H and Cl atoms.

Supplementary material

CCDC 674229 and 674230 contain the supplementary crystallographic data for compounds **1a** and **2b**. These data can be obtained free of charge from The Cambridge Crystallographic Data Centre via www.ccdc.cam.ac.uk/data_request/cif.

Acknowledgements

Financial support by the National Science Foundation of China (20531020, 20721063, 20771028), by Shanghai Leading Academic Discipline project (B108) and by Shanghai Science and Technology Committee (06XD14002) is gratefully acknowledged.

References

[1] (a) A.D. Phillips, G. Laurenczy, R. Scopelliti, P.J. Dyson, Organometallics 26 (2007) 1120;
(b) S. Liu, Y.-F. Han, G.-X. Jin, Chem. Soc. Rev. 36 (2007) 1543;
(c) X. Wang, G.-X. Jin, Chem. Eur. J. 11 (2005) 5758.
[2] V. Leeuwen, Homogeneous Catalysis: Understanding the Art, Kluwer Academic, Dordrecht, The Netherlands, 2004.
[3] (a) M. Cheng, E.B. Lobkovsky, G.W. Coates, J. Am. Chem. Soc. 120 (1998) 11018;
(b) P.L. Holland, W.B. Tolman, J. Am. Chem. Soc. 121 (1999) 7270;
(c) C. Cui, H.W. Roesky, H.G. Schmidt, M. Noltemeyer, H. Hao, F. Cimpoesu, Angew. Chem., Int. Ed. 39 (2000) 4274;
(d) V.C. Gibson, J.A. Segal, J.P. White, D.J. Williams, J. Am. Chem. Soc. 122 (2000) 7120;
(e) N.J. Hardman, C. Cui, H.W. Roesky, W.H. Fink, P.P. Power, Angew. Chem., Int. Ed. 40 (2001) 2172;
(f) H. Andres, E. Bominaar, J.M. Smith, N.A. Eckert, P.L. Holland, E. Münck, J. Am. Chem. Soc. 124 (2002) 3012;
(g) A. Panda, M. Stender, R.J. Wright, M.M. Olmstead, P. Klavins, P.P. Power, Inorg. Chem. 41 (2002) 3909;
(h) N.A. Eckert, E.M. Bones, R.J. Lachicotte, P.L. Holland, Inorg. Chem. 42 (2003) 1720;
(i) A.P. Dove, V.C. Gibson, P. Hormnirun, E.L. Marshall, J.A. Segal, A.J.P. White, D.J. Williams, Dalton Trans. (2003) 3088;
(j) N.A. Eckert, J.M. Smith, R.J. Lachicotte, P.L. Holland, Inorg. Chem. 43 (2004) 3306;
(k) E.A. Gregory, R.J. Lachicotte, P.L. Holland, Organometallics 24 (2005) 1803;
(l) J. Vela, J.M. Smith, Y. Yu, N.A. Ketterer, C.J. Flaschenriem, R.J. Lachicotte, P.L. Holland, J. Am. Chem. Soc. 127 (2005) 7857;
(m) M. Susan, Kloek, K.I. Goldberg, J. Am. Chem. Soc. 129 (2007) 3460;
(n) L. Bourget-Merle, M.F. Lappert, J.R. Severn, Chem. Rev. 102 (2002) 3031.
[4] (a) P.G. Hayes, G.C. Welch, D.J.H. Emslie, C.L. Noack, W.E. Piers, M. Parvez, Organometallics 22 (2003) 1577;
(b) H.Y. Gao, W.J. Guo, F. Bao, G.Q. Gui, J.K. Zhang, F.M. Zhu, Q. Wu, Organometallics 23 (2004) 6273;
(c) A.M. Reynolds, B.F. Gherman, C.J. Cramer, W.B. Tolman, Inorg. Chem. 44 (2005) 6989;
(d) B.Y. Lee, H.Y. Kwon, S.Y. Lee, S.J. Na, S. Han, H. Yun, H. Lee, Y.W. Park, J. Am. Chem. Soc. 127 (2005) 3031;
(e) X. M Liu, H. Xia, W. Gao, L. Ye, Y. Mu, Q. Su, Y. Ren, Eur. J. Inorg. Chem. (2006) 1216;
(f) X.M. Liu, W. Gao, Y. Mu, G.H. Li, L. Ye, H. Xia, Y. Ren, S.H. Feng, Organometallics 24 (2005) 1614;
(g) Y.M. Badiei, A. Krishnaswamy, M.M. Melzer, T.H. Warren, J. Am. Chem. Soc. 12 (2006) 15056;
(h) E.C. Brown, I.B. Nahum, J.T. York, N.W. Aboelella, W.B. Tolman, Inorg. Chem. 46 (2007) 486;
(i) Y. Ren, X.M. Liu, W. Gao, H. Xia, L. Ye, Y. Mu, Eur. J. Inorg. Chem. (2007) 1808.
[5] (a) G. Bhalla, X.Y. Liu, J. Oxgaard, W.A. Goddard, R.A. Periana, J. Am. Chem. Soc. 127 (2005) 11372;
(b) Y. Guari, S.S. Etienne, B. Chaudret, Eur. J. Inorg. Chem. (1999) 1047;
(c) F.C.C. Mouraa, E.N. Santosa, R.M. Lagoa, M.D. Vargasb, M.H. Araujoa, J. Mol. Catal. A: Chem. 226 (2005) 243;
(d) L. Flores-Santos, E. Martin, A. Aghmiz, M. Dieguez, C. Claver, M. Masdeu-Bulto, M.A. Munoz-Hernandez, Eur. J. Inorg. Chem. (2005) 2315;
(e) G. Bhalla, J. Oxgaard, W.A. Goddard, R.A. Periana, Organometallics 24 (2005) 5499;
(f) G. Bhalla, J. Oxgaard, W.A. Goddard, R.A. Periana, Organometallics 24 (2005) 3229;
(g) V.R. Landaeta, B.K. Munoz, M. Peruzzini, V. Herrera, C. Bianchini, R.A. Sanchez-Delgado, Organometallics 25 (2006) 403;
(h) B.A. Messerle, K.Q. Vuong, Organometallics 26 (2007) 3031;
(i) K.D. Hesp, D. Wechsler, J. Cipot, A. Myers, R. McDonald, M.J. Ferguson, G. Schatte, M. Stradiotto, Organometallics 26 (2007) 5430;
(j) E. Peris, R.H. Crabtree, Coord. Chem. Rev. 248 (2004) 2239;
(k) D.J. Weix, J.F. Hartwig, J. Am. Chem. Soc. 129 (2007) 7720.
[6] H.Y. Wang, X. Meng, G.-X. Jin, Dalton Trans. (2006) 2579.
[7] D. Carmona, M.P. Lamata, F. Viguri, R. Rodriguez, F.J. Lahoz, I.T. Dobrinovitch, L.A. Oro, Dalton Trans. (2007) 1911.
[8] F. Hanasaka, Y. Tanabe, K. Fujita, R. Yamaguchi, Organometallics 25 (2006) 826.
[9] C. Pettinari, R. Pettinari, F. Marchetti, A. Macchioni, D. Zuccaccia, B.W. Skelton, A.H. White, Inorg. Chem. 46 (2007) 896.
[10] Q. Zhao, S.J. Liu, M. Shi, C.M. Wang, M.X. Yu, L. Li, F.Y. Li, T. Yi, C.H. Huang, Inorg. Chem. 45 (2006) 6152.
[11] (a) A.J. Wilkinson, H. Puschmann, J.A.K. Howard, C.E. Foster, J.A.G. Williams, Inorg. Chem. 45 (2006) 10230;
(b) V.A. Bhirud, A. Uzun, P.W. Kletnieks, R. Craciun, J.F. Haw, D.A. Dixon, M.M. Olmstead, B.C. Gates, J. Organmet. Chem. 692 (2007) 2107;
(c) O. Siri, J.P. Taquet, J.P. Collin, M.M. Rohmer, M. Bonard, P. Braunstein, Chem. Eur. J. 11 (2005) 7247.
[12] G.M. Sheldrick, SHELXL-97, Universität Gtötingen, Germany, 1997.